

Jonathan A. Olivier
e-mail: jonathan.olivier@up.ac.za

Leon Liebenberg
e-mail: lieb@up.ac.za

Department of Mechanical and Aeronautical
Engineering,
University of Pretoria,
Pretoria, 0002, South Africa

Mark A. Kedzierski
e-mail: mark.kedzierski@nist.gov
National Institute of Standards and Technology,
Gaithersburg, MD

Josua P. Meyer*
e-mail: jmeyer@up.ac.za
Department of Mechanical and Aeronautical
Engineering,
University of Pretoria,
Pretoria, 0002, South Africa

Pressure Drop During Refrigerant Condensation Inside Horizontal Smooth, Helical Microfin, and Herringbone Microfin Tubes

This paper presents a study of pressure drops during condensation inside a smooth, an 18-deg helical microfin, and a herringbone microfin tube. Measurements were conducted with refrigerant flowing through the tube of a concentric heat exchanger, with water flowing in a counterflow direction in the annulus. Each tube was part of a condenser consisting of eight subcondensers with instrumentation preceding each subcondenser. Three refrigerants were used, namely, R-22, R-407C, and R-134a, all operating at a saturation temperature of 40 °C with mass fluxes ranging from 400 to 800 kg/m² s. Inlet qualities ranged from 0.85 to 0.95 and outlet qualities ranged from 0.05 to 0.15. The test results showed that on average for the three refrigerants the pressure gradients of the herringbone microfin tube were about 79% higher than that of the smooth tube and about 27% higher than that of the helical microfin tube. Further, a correlation from the literature for predicting pressure drops inside a helical microfin tube was modified from the herringbone microfin tube. The modified correlation predicted the data to within an error of 1% and had an absolute mean deviation of 6.8%. This modified correlation compared well with a correlation from the literature that predicted the data to within an error of 7%. [DOI: 10.1115/1.1795240]

Keywords: Refrigerant Condensation, Smooth Tube, Helical Microfin Tube, Herringbone Microfin Tube, Pressure Drop, Flow Regime

Introduction

Many types of augmentation techniques exist today, with tubes having internal microfins being most common. A study conducted by Liebenberg [1], using helical microfin tubes with an inner diameter of 8.9 mm, showed that these tubes have a heat transfer coefficient increase of about 200% compared to that of a smooth tube. With this increase in heat transfer coefficients, however, there was also an increase in pressure drop. It was found, on average, that this increase was about 100% higher than that inside a smooth tube. These pressure drops were attributed to the increased vapor velocities in a helical microfin tube condenser, brought about by the greater regions of annular flow, which in turn increases the turbulence inside the tube compared to a smooth tube [1]. The fins redistribute the liquid layer around the circumference of the tube, forcing the flow to become annular rather than intermittent or stratified.

In the mid-1990s a new generation of microfin tube was being developed, one of them being the herringbone microfin tube. This tube consists of a double V-groove, as shown in Fig. 1(a), with grooves embossed on the inner surface. The orientation was chosen such that the liquid would converge at the top and bottom of the tube and diverge at the sides [Fig. 1(b)]. Due to the effect of gravity, especially at low velocities, the distribution of liquid at the bottom of the tube will be higher than at the top. The heat transfer enhancement, as explained by Miyara et al. [2], is due to the thin film layer on the sides and the mixing of the converging liquid at the top and bottom of the tube.

Table 1 gives a short summary of the experimental conditions used in previous work [3–5] on herringbone microfin tubes. The

mass fluxes ranged from 100 to 400 kg/m² s and in some cases are lower than required for heat-pump water-heater applications where the mass fluxes range up to 1000 kg/m² s. Although smaller tubes are being investigated by other researchers, especially in countries such as the US and Asia where tube diameters as low as 4 mm are being introduced, 3/8 in. (~9.5 mm) tubes are still the most common tubes used in residential and commercial air conditioners, heat pumps, and refrigeration systems.

The objective of this paper is to first introduce experimental findings of condensation pressure drops inside herringbone microfin tubes at mass fluxes higher than were published before (400–800 kg/m² s) and inside tubes with larger diameters (8.5 mm inside and 9.53 mm outside). The second objective is to compare the experimental data of the herringbone microfin tube to experimental data on smooth and helical microfin tubes. Third, the pressure-drop data were used to develop a modified pressure-drop correlation for a herringbone microfin tube.

Experimental Facility

The experimental test facility consisted of two main sub-systems: the vapor-compression loop and the water loops. A schematic of the experimental setup is given in Fig. 2. Each of the sub-systems was of the closed-loop type. The vapor-compression loop consisted of a hermetically sealed reciprocating compressor having a nominal cooling capacity of 9.6 kW, an oil separator with a maximum discharge volume of 2.6 m³/h, a manually adjustable expansion valve, a water-heated evaporator, and a water-cooled test condenser. Three test condensers were used, namely, a smooth tube, an 18-deg helical microfin tube, and a herringbone microfin tube. Geometric parameters of the tubes as well as their lengths are given in Table 2. The lengths of the tubes were chosen to obtain an energy balance better than 1%. The orientation of the herringbone microfin tube was chosen such that the liquid converges at the top and bottom of the tube and diverges at the sides.

*Corresponding author.

Contributed by the Heat Transfer Division for publication in the JOURNAL OF HEAT TRANSFER. Manuscript received by the Heat Transfer Division November 19, 2003; revision received June 15, 2004. Associate Editor: M. Jensen.

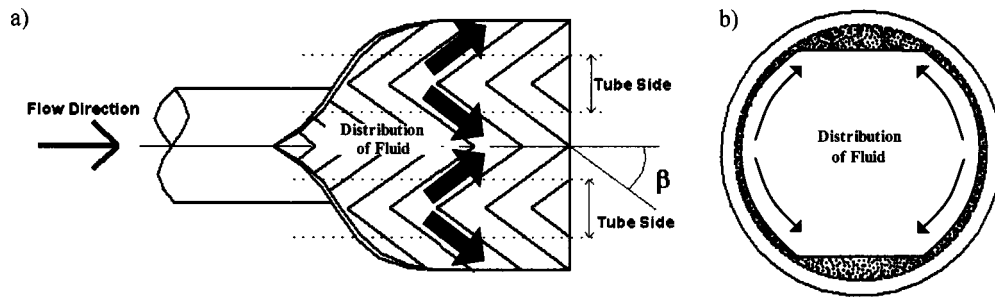


Fig. 1 a) Basic geometry of the herringbone microfin tube (not to scale) and b) an illustration of how condensate is distributed inside the tube for the adopted orientation (exaggerated)

Visual inspection ensured that the orientation of each tube was maintained during the manufacture of the condenser. Sight glasses, cylindrical in shape, were used to visualize the flow patterns inside the tubes. The inner diameter of these sight glasses was the same as the inner diameter of the condenser tubes. This was done so that the flow inside the tubes would not be affected.

The test condenser was of the tube-in-tube type with refrigerant flowing in the inner tube and water flowing in a counterflow direction in the annulus. The cold and hot water loops were connected to the condenser and evaporator, respectively. On the condensing side the cold water was used as a heat sink, removing the latent heat from the condensing refrigerant. The water temperature was kept constant in the range of 20–25°C (depending on the experiments conducted) in a 1000 l insulated reservoir connected to a 15 kW chiller. The water gauge pressure in the annulus was maintained between 70 and 140 kPa to prevent the formation of air bubbles, which could affect temperature readings and the heat transfer from the refrigerant to the water. A centrifugal pump pumped the chilled water to the double-tube condenser. A hand-controlled valve controlled the water flow rate through the test sections. After passing through the condenser, the water returned to the reservoir of the chiller unit.

A similar hot water flow loop was used on the evaporating side, also with an insulated 1000 l reservoir, but connected to a 12 kW electric resistance heater. The reservoir water temperature was varied between 30°C and 40°C depending on the experiments conducted. Increasing or decreasing the temperature of the water through the evaporator altered the refrigerant density at the compressor inlet and thus the refrigerant mass flow.

For the smooth and helical microfin tube, two resistance temperature detectors (RTDs) were used prior to each subsection, placed at the top and bottom of the inner tube. This was done to obtain an average temperature of the tube since the distribution of the liquid layer inside the tube would under- or overestimate the temperature measurement if only one RTD were used. For the herringbone microfin tube, however, the RTDs were placed at the top and on the side of the inner tube because the liquid film thickness on the top is much thicker than on the side. The absolute pressures of the condensing refrigerant were measured with piezoelectric pressure transducers, which were positioned at the inlet of each condenser subsection. Two Coriolis mass flow metres were used for the vapor compression loop and the cold-water loop. The

uncertainties of the instruments, given in Table 3, were calculated by using the method of Kline and McClintock [6].

Data Reduction

Deduction of Vapor Quality. The properties of the refrigerant at the inlet and outlet of the condenser were determined by temperature and pressure measurements. From these measurements the thermophysical properties of the condensing refrigerant were determined by interpolating the superheated (at the inlet of the condenser) and subcooled (at the outlet of the condenser) tables that were obtained from REFPROP [7]. The refrigerant properties for the rest of the condenser (two-phase sections) were determined by assuming that the calculated values of the heat transferred to the water was more accurate than the values calculated for the refrigerant. With this assumption the enthalpy values of the refrigerant could be deduced. In the first test subsection the water heat flux was equated to the refrigerant heat flux (due to the refrigerant enthalpy change) to obtain the outlet enthalpy h_o . This outlet enthalpy was then used as the inlet enthalpy h_i for the next subsection. This procedure was repeated for all eight subsections [1].

The average sectional vapor quality was thus obtained by

$$x_i = \frac{h_i - h_L}{h_L - h_V} \text{ with } h_L \text{ and } h_V \text{ measured at } T_i$$

$$x_o = \frac{h_o - h_L}{h_L - h_V} \text{ with } h_L \text{ and } h_V \text{ measured at } T_o \quad (1)$$

The average vapor quality of each test subsection was then determined as

$$x = \frac{x_i + x_o}{2} \quad (2)$$

Pressure Drop and Pressure Gradients. The total pressure drop was defined as

$$\Delta p_i = \Delta p_m + \Delta p_f + \Delta p_g \quad (3)$$

where the momentum pressure drop Δp_m is defined as

Table 1 Experimental conditions of previous work done on herringbone microfin tubes

	Ebisu and Torikoshi [3]	Miyara et al. [4]	Goto et al. [5]
Tube inside diameter [mm]	7	7	8
Total condenser length [m]	0.54	4	2
Refrigerant	R-22, R-407C	R-22, R-410A	R-22, R-410A
Saturation temperature [°C]	50	40	40
Mass flux range [kg/m ² s]	150–400	100–400	200–340
Pressure-drop measurements	Local	Average	Average
Correlation	No	Yes	No

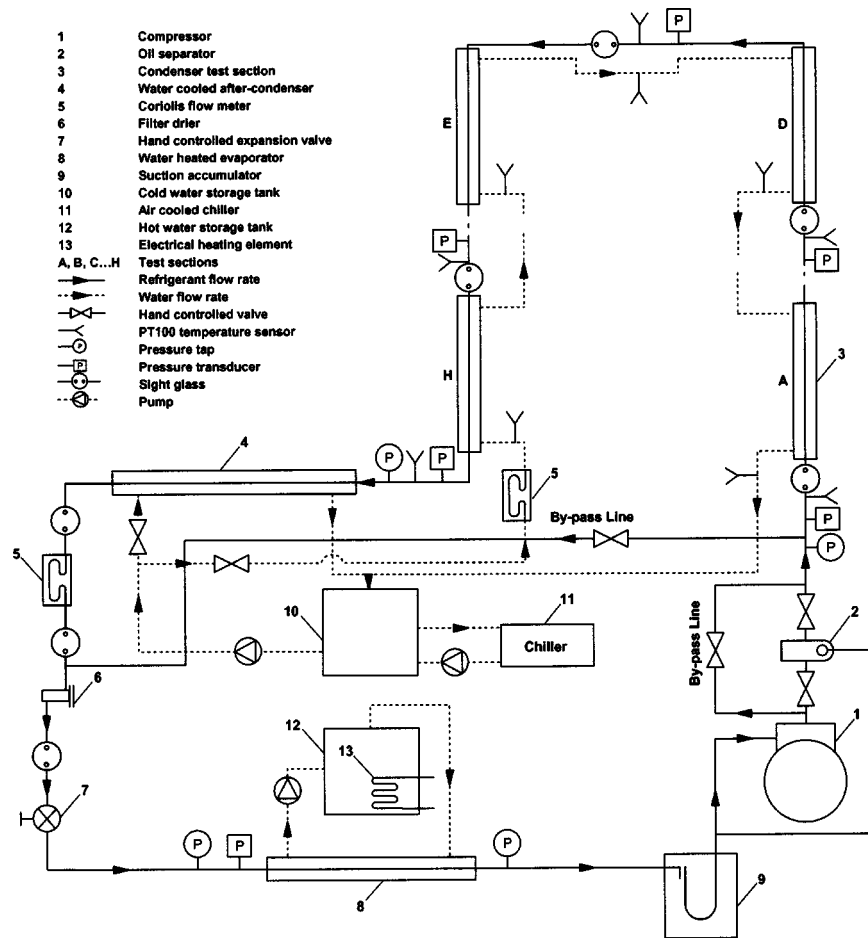


Fig. 2 Schematic of the experimental facility

$$\Delta p_m = G^2 \left\{ \left[\frac{(1-x)^2}{\rho_L(1-\varepsilon)} + \frac{x^2}{\rho_V \varepsilon} \right]_{out} - \left[\frac{(1-x)^2}{\rho_L(1-\varepsilon)} + \frac{x^2}{\rho_V \varepsilon} \right]_{in} \right\} \quad (4)$$

The void fraction ε used was that given by Rouhani and Axelsson [8]. Since the tubes were horizontally positioned, the gravitational pressure drop Δp_g was neglected. The frictional pressure drop Δp_f was calculated from known correlations obtained in the literature.

The measured pressure between each subsection that was in a two-phase region was subtracted from each other to obtain the total experimental pressure drop per subsection. This in turn was divided by the subsection length to obtain the pressure drop per unit condenser length, or the pressure gradient.

Penalty Factor. The parameter used to compare the pressure-drop characteristics of the herringbone microfin tubes to those of

Table 2 Inner tube geometric parameters of the test condensers

Type	Smooth	Helical	Herringbone
Material	Hard-drawn copper	Hard-drawn copper	Soft-drawn copper
Helix angle, β [°]	-	18	16
Apex angle, γ [°]	-	40	25
Number of fins, n [-]	-	60	70
Fin base thickness, t_b [mm]	-	1.672	0.0887
Outside diameter, D_o [mm]	9.52	9.55	9.51
Inside diameter, D_i [mm]	8.11	8.94	8.52
Tube wall thickness, t_w [mm]	1.4	0.307	0.3
Equivalent diameter, D_e [mm]	8.11	8.79	8.82
Fin height, e [mm]	-	0.209	0.2
Actual flow area, A_{fa} [m ²]	51.7×10^{-6}	60.64×10^{-6}	61.16×10^{-6}
Condenser subsection length [m]	1.5	1.13	0.563
Condenser total length [m]	12	9	4.5

Table 3 Estimated 95% uncertainties for the experimental instrumentation and Eq. (9) data

Measurements	Uncertainty
Refrigerant temperature	0.14 K
Water temperature	0.11 K
Saturation temperature	0.12 K
Pressure	0.23%
Refrigerant mass flow rate	0.23%
Water mass flow rate	0.28%
Average quality	3.02%
Viscosity	0.10%
Density	0.03%
Re	1.02%
X_{tt}	3.82%
Φ_L	4.46%
Δp_{Lo}	4.80%
Δp	6.80%

the smooth and helical microfin tube is the penalty factor PF . The penalty factor is defined as the ratio of the measured total pressure gradient in the herringbone microfin tube to the measured total pressure gradient in the smooth tube [Eq. (5)] and the ratio of the measured total pressure gradient in the herringbone microfin tube to the measured total pressure gradient in the helical microfin [Eq. (6)] as follows:

$$PF = \left(\frac{\Delta p_h}{\Delta p_s} \right) \quad (5)$$

$$PF = \left(\frac{\Delta p_h}{\Delta p_{he}} \right) \quad (6)$$

Flow Regimes. With the aid of mini digital video cameras and the flow regime maps developed by Thome [9], flow patterns were identified within the tubes, thus allowing the determination of flow regime transitions. The Froude rate, defined as

$$Ft = \left[\frac{G^2 x^3}{(1-x)\rho_v^2 g D_i} \right]^{1/2} \quad (7)$$

which is essentially the ratio relating the kinetic energy of the vapor to the amount of energy required to pump the liquid from the bottom to the top of the tube. In regions where gravitational drag becomes dominant, the Froude rate expresses how the energy dissipation due to liquid waves and liquid mass movement around the tube's diameter are related to the energy in the flow stream [1].

Experimental Results

Prior to obtaining experimental data on the herringbone microfin tube, experiments were conducted on the smooth and helical microfin tubes. These data were compared to pressure-drop correlations obtained from the literature. For the smooth tube the pressure-drop data were predicted on average for the three refrigerants to within 33% using the correlation of Lockhart and Martinelli [10]. The correlation of Cavallini et al. [11] was used for the helical microfin tube and predicted the pressure-drop data to within 13%.

Figure 3 shows the use of the flow regime maps of Thome [9]. For the smooth tube, the transition quality was calculated in the manner described by Thome [9] and is given in Fig. 3(a). This method was, however, only applicable for smooth tubes, and a new method needed to be developed for the helical and herringbone microfin tubes. The method used by Liebenberg [1] for determining the transition quality was implemented for the smooth tube, and the results differed by a quality of as little as 0.001. This meant that this new method could be used for the helical and herringbone microfin tubes. The flow regime maps for the helical and herringbone microfin tubes are given in Figs. 3(b) and 3(c). In these maps the transition quality from annular to intermittent

flow is different for each tube; the smooth tube having the highest transition quality and the herringbone microfin tube having the lowest.

Figure 4 shows a summary of the pressure gradients for the three refrigerants inside the smooth, helical microfin and herringbone microfin tubes as a function of the average vapor quality at mass fluxes of 400, 600, and 800 kg/m² s. The overall trend for the three refrigerants is that the pressure gradients increase with an increase in vapor quality. At high qualities where the pressure gradients are the highest, the flow was found to be annular, implying that the main reason for the drop in pressure was due to the increased turbulence formed by the high-velocity vapor-generating friction against the liquid annulus. Looking at Eq. (7), the Froude rate has a high value for high qualities, and thus, the flow is shear dominated. As the quality decreases a transition starts to occur between annular and intermittent flow and the vapor and liquid velocities become similar. For this reason the pressure gradients are much lower and from Eq. (7) the Froude rate has a small value, implying that the flow is gravity dominated.

For the smooth tube this transition region occurred at a quality of about 50% [12]. For the helical microfin and herringbone microfin tubes the transition occurred at a quality of 28% and 26% [12,13], respectively. This is characterized by a sharp increase in pressure gradient at qualities higher than the transition qualities. Thus, for the helical and herringbone microfin tubes, due to the increased turbulence generated by the fins, annular flow occurs over a larger vapor-quality region than for the smooth tube. This is visually shown in Table 4 from the captured video images. Looking at a quality of about 0.46, for the smooth tube the flow is intermittent, with slugs and plugs forming at the top of the tube, while the helical and herringbone microfin tubes are still in annular flow, noting that there is a liquid film layer around the circumference of the tube. This implies that the fins redistribute the liquid around the circumference of the tube, extending the annular flow regime down to lower qualities. This further implies that the average pressure gradients for these tubes will be higher due to the increase in turbulence found in annular flow. Since the transition quality for the herringbone microfin tube is lower than that of the helical microfin tube, one can expect the overall pressure drops (on average) for the herringbone microfin tube to be higher.

Figure 5 shows a summary of the average pressure gradients for condensation as a function of the mass flux. The overall trend is that the pressure gradients increase with an increase in mass flux. Further, it is noted that the local pressure gradients (Fig. 4) and the average pressure gradients (Fig. 5) of R-134a are always higher than that of R-22 and R-407C, with R-407C being the lowest. This concurs with expectations, as R-134a is a low-pressure refrigerant, which implies higher vapor velocities, resulting in higher relative pressure drops than those for the higher-pressure refrigerant.

Comparisons of Pressure-Drop Penalty Factors

The penalty factors for the herringbone microfin tube were determined by analyzing the ratio of the pressure drops of the herringbone microfin tube to the pressure drops of the smooth [Eq. (3)] and helical microfin tubes [Eq. (4)], reduced to equivalent lengths. The plots of the penalty factors are given in Fig. 6. For the plots against the smooth tube, Fig. 6(a), the penalty factors are always greater than one throughout the mass flux range, implying that the herringbone microfin tube overall has a higher pressure drop than that of the smooth tube. On average, when using R-22, the pressure drop is 84% higher than in the smooth tube, while when using R-407C and R-134a the pressure drops are 80% and 72% higher, respectively. On average for the three refrigerants the herringbone microfin tube has a 79% higher pressure drop than that of the smooth tube. This increase is due to the increase in turbulence generated by the fins. As was explained previously, the fins extend the annular flow regime to lower qualities by redistributing the liquid around the circumference of the tube. This is also shown visually in Table 4.

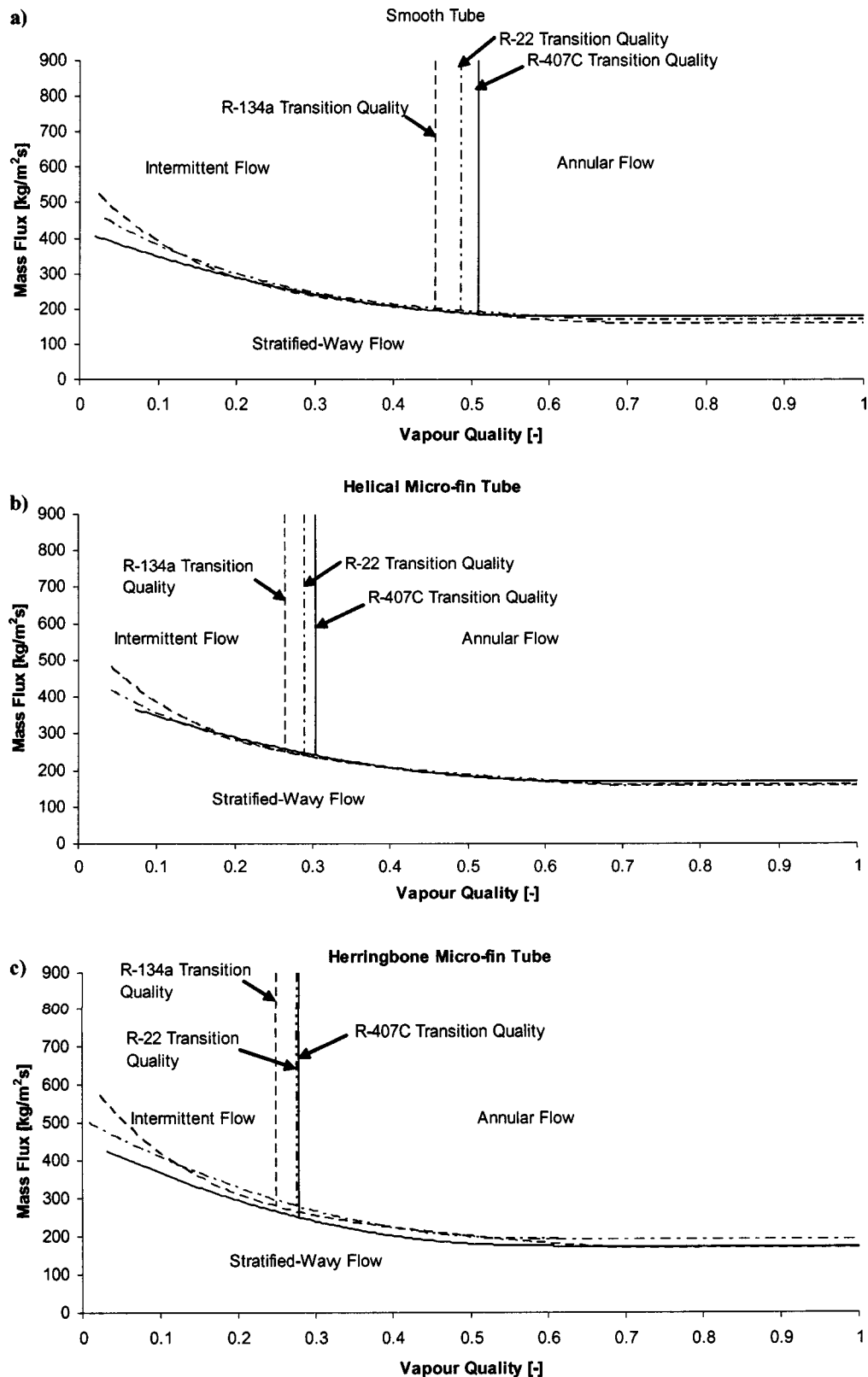


Fig. 3 Determining the transition qualities by making use of a) the Thome [9] map for the smooth tube, and the method used by Liebenberg et al. [13] for b) the helical microfin tube and c) the herringbone microfin tube

The penalty factors for the herringbone microfin tube against that of the helical microfin tube are given in Fig. 6(b). For R-22 the pressure drops of the herringbone microfin tube are about 41% higher than that of the helical microfin tube. This agrees well with

the work of other researchers [2–5,8]. For R-407C and R-134a, however, the penalty factors at lower mass fluxes (400–500 kg/m² s) are below one. An explanation is that the flow over the fins, as explained by Wang et al. [14], induces a viscous

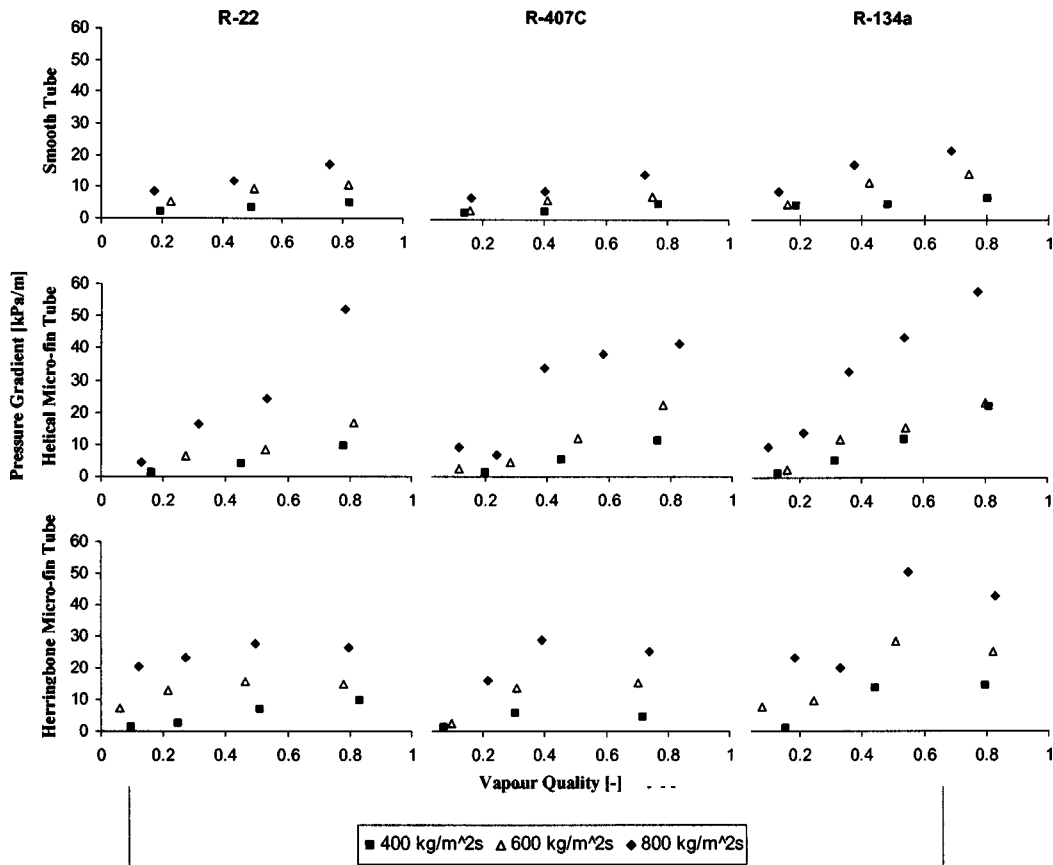


Fig. 4 Pressure gradients at mass fluxes of 400, 600, and 800 kg/m² s for the three tubes and refrigerants tested

sublayer thickness, buffer layer, and an integral constant in the log-law that is greater than that for the helical microfin tube, implying that the fins might have a drag reduction effect when compared to the helical microfin tube. At higher mass fluxes the pressure drops for these two refrigerants are, respectively, about 17% and 24% higher. On average for the three refrigerants the pressure drops of the herringbone microfin tube are about 27% higher than those of the helical microfin tube.

Comparisons With Other Pressure-Drop Correlations

Figure 5 gives plots of the correlation of Miyara et al. [4] with regard to the herringbone microfin tube experimental data. The deviations were calculated by

$$\text{Mean Deviation (\%)} = \frac{\Delta p_{pd} - \Delta p_{ex}}{\Delta p_{ex}} \times 100 \quad (8)$$

The experiments of Miyara et al. [4] were conducted at low mass fluxes (100 to 400 kg/m² s) with refrigerants R-22 and R-410A (see Table 1), also from where they derived their correlation. From Fig. 4 it follows that the correlation slightly deviates from the data at high mass fluxes, especially for R-407C and R-134a. On average, however, this correlation only underpredicted the data by 7%, implying that it could be used at mass fluxes higher than 400 kg/m² s and maybe even for refrigerants other than R-22 and R-410A.

Modification of a Pressure-Drop Correlation

The correlation developed by Carnavos [15] for finned tubes was modified for the herringbone microfin tube. The pressure drop due to friction is given by the product of the liquid-only pressure drop and a two-phase multiplier

$$\Delta p_f = \Delta p_{Lo} \Phi_L^2 \quad (9)$$

with the two-phase multiplier being that of Souza and Pimenta [16],

$$\Phi_L^2 = 1.376 + \frac{7.242}{X_{tt}^{1.655}} \quad (10)$$

The modified Darcy-Weisbach equation as obtained from Friedel [17] was calculated by

$$\Delta p_{Lo} = \frac{2 f_{Lo} G^2 (1-x)^2 L}{\rho_L D_i} \quad (11)$$

The liquid-only friction factor, as given by Carnavos [15] for a finned tube

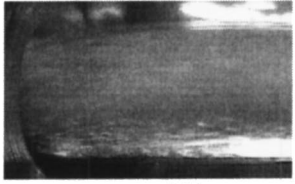
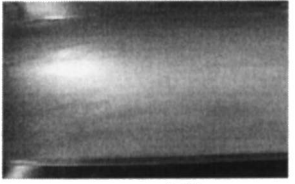
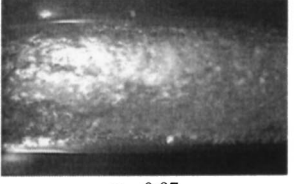
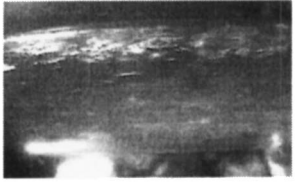
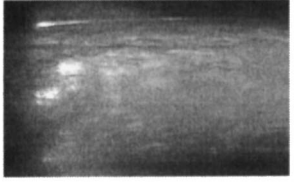
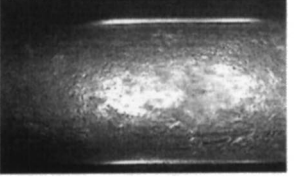
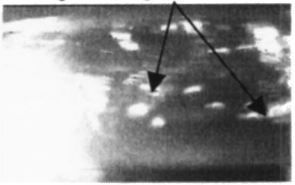
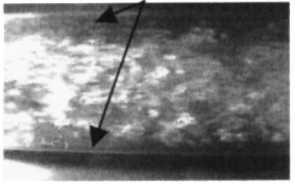
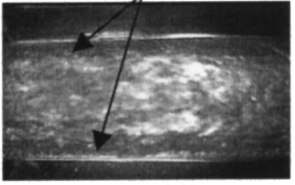
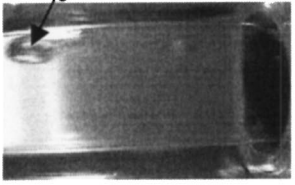
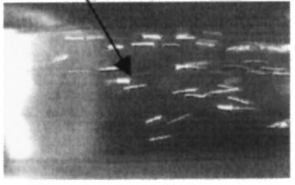
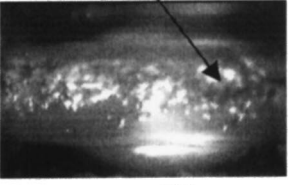
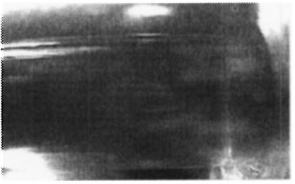
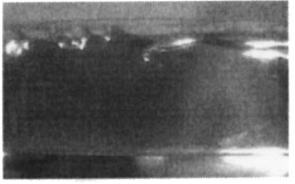

$$f_{Lo} = 0.046 \text{Re}_L^{-0.2} \left(\frac{D_i}{D_e} \right) \left(\frac{A}{A_n} \right)^{0.5} (\sec \beta)^{0.75} \quad (12)$$

with D_e being the equivalent inner tube diameter taking the fins into account, D_i the fin-root diameter, A_n the nominal flow area based on the fin-root diameter, and A the actual cross-sectional flow area of the tube. The area ratio for the microfin tube as given by Azer and Said [18] is

$$\frac{A}{A_n} = 1 - \frac{4ent}{\pi D_i^2 \cos \beta} \quad (13)$$

with e being the fin height, n the number of fins, t the fin thickness, and β the helix angle of the fins. The terms $\sec \beta$ and $\cos \beta$ in Eqs. (12) and (13) account for the swirling effect induced by the fins inside the helical microfin tube. By multiplying the cos

Table 4 Images of R-134a condensing at a mass flux of 500 kg/m² s for the three tubes tested

	Smooth Tube	Helical Micro-fin Tube	Herringbone Micro-fin Tube
	 x = 0.96	 x = 0.97	 x = 0.97
	 x = 0.77	 x = 0.79	 x = 0.79
↓ Decreasing Quality [-]	Plugs and Slugs  x = 0.46	Thick liquid film  x = 0.48	Thick liquid film  x = 0.46
	Plug flow  x = 0.21	Swirling of slugs and plugs  x = 0.20	Chaotic behaviour of slugs and plugs  x = 0.23
	 x = 0.06	 x = 0.06	Plug flow at very low quality  x = 0.06

and sec terms by a factor 2 and changing the power of the sec term in Eq. (12) from 0.75 to 1.1, the equations become, respectively,

$$f_{Lo} = 0.046 \text{Re}_L^{-0.2} \left(\frac{D_i}{D_e} \right) \left(\frac{A}{A_n} \right)^{0.5} (2 \sec \beta)^{1.1} \quad (14)$$

$$\frac{A}{A_n} = 1 - \frac{2ent}{\pi D_i^2 \cos \beta} \quad (15)$$

The experimental pressure-drop data using the modified correlation were predicted to within an error of 1%, having an absolute mean deviation of 6.8%; 94% of the data were predicted within ± 20%. This is visually shown in Fig. 7. The modified correlation is also visualized with the experimental data in Fig. 4. The uncertainties of Eq. (9) are given in Table 3.

To summarize, Eqs. (14) and (15) can be given in a more general form as follows:

$$f_{Lo} = 0.046 \text{Re}_L^{-0.2} \left(\frac{D_i}{D_e} \right) \left(1 - \frac{Xent}{\pi D_i^2 \cos \beta} \right)^{0.5} (X \sec \beta)^Y$$

For helical microfin tubes:

$$X = 1$$

$$Y = 0.75$$

$$(16)$$

For herringbone microfin tubes:

$$X = 2$$

$$Y = 1.1$$

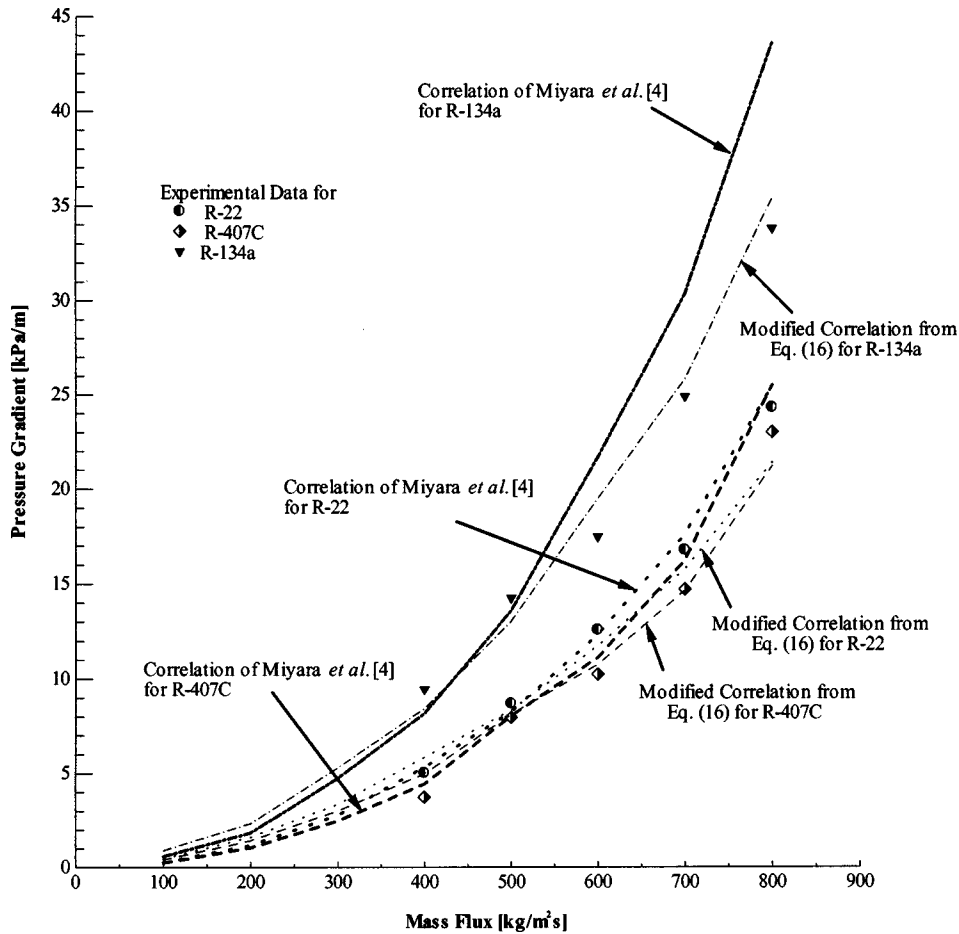


Fig. 5 Average pressure drops of the experimental data and that predicted by Miyara et al. [4] and the newly developed correlation for refrigerants R-22, R-407C, and R-134a

When comparing the proposed correlation with that of Miyara et al. [4] in Fig. 5, at high-mass fluxes the two differ by as much as 19%, but seem to converge to a point as the mass flux decreases. This is due to the fact that both correlations are strongly dependant on the mass flux. Further, the correlation of Miyara et al. [4] at high mass fluxes predicts higher pressure drops than the proposed correlation. This, however, changes from a mass flux lower than $500 \text{ kg/m}^2 \text{ s}$ where the proposed correlation predicts higher pressure drops. It is also noted that the two correlations are similar in form; the correlation of Miyara et al. [4] is defined in terms of a vapor-only pressure drop multiplied by a modified form of the Haraguchi et al. [19] two-phase multiplier.

Conclusion

Experiments for refrigerant pressure drops were conducted with herringbone microfin tubes during condensation and compared with the performance of their smooth and helical microfin counterparts. The condensers were of the tube-in-tube type with the refrigerant flowing in the inner tube and cooling water in a counterflow direction in the annulus. Three refrigerants were tested, namely, R-22, R-134a, and R-407C. All tests were conducted at a nominal saturation temperature of 40°C and at mass fluxes ranging from 400 to $800 \text{ kg/m}^2 \text{ s}$.

The results showed that for all three test condensers the pressure gradients increased with an increase in quality. The trends of the pressure gradients were due to the increase in turbulence from the intermittent to the annular region. These transitions occurred at an average vapor quality of 50%, 28%, and 26% for the smooth, helical microfin, and herringbone microfin tubes, respec-

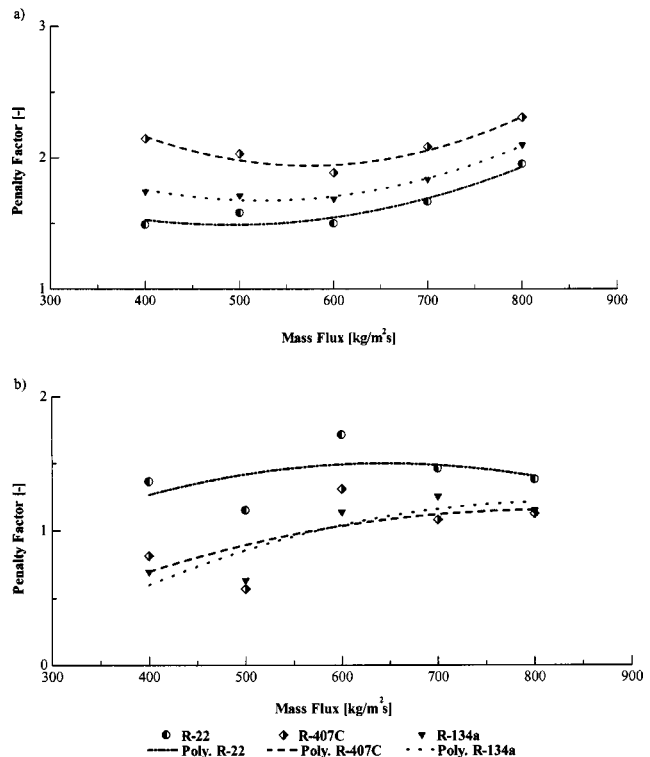


Fig. 6 Penalty factors for the herringbone microfin tube against a) the smooth tube and b) the helical microfin tube for R-22, R-407C, and R-134a

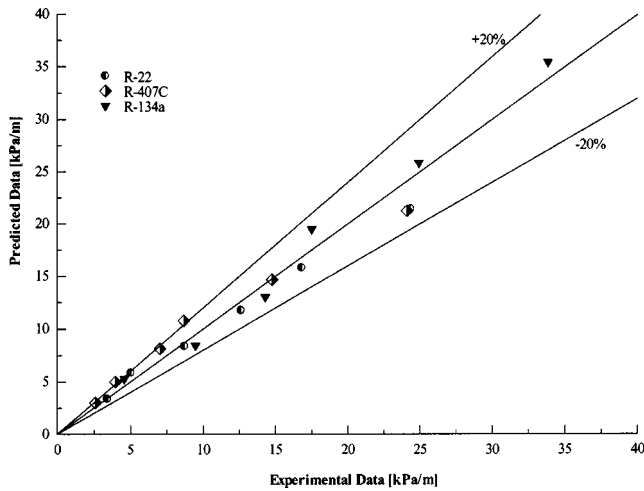


Fig. 7 Comparison of the experimental data with the modified prediction data for R-22, R-407C and R-134a

tively. The high pressure gradients, found at the high-quality regions (above the transition qualities), were due to the friction generated during annular flow by the high-velocity vapor core against the slow-moving liquid annulus. At low qualities where the flow was intermittent (below the transition qualities), and thus gravity dominated, the pressure gradients were lower and remained more or less constant. It was concluded that the fins on both the helical and herringbone microfin tubes redistributed the liquid layer around the circumference of the tube, extending the annular flow regime to lower qualities, thus having a longer range in which the flow is very turbulent.

With the pressure-drop data, the penalty factors of the herringbone microfin tube against that of the smooth and helical microfin tubes were calculated. The results indicated that, for the herringbone microfin tube against the smooth tube, the penalty factors were always above one. On average the pressure drops of the herringbone microfin tube were about 79% higher than those of the smooth tube. Results also indicated that the penalty factors for the three refrigerants were almost the same.

For the herringbone microfin tube against the helical microfin tube, the penalty factors for R-407C and R-134a were less than one for low mass fluxes. An explanation for this is that the fins might have a drag-reducing effect due to a larger viscous sublayer thickness, buffer layer, and a greater integral constant in the log-law. For R-22, however, the penalty factors were, on average, greater than one. For the three refrigerants, the pressure drops were, on average, about 27% higher.

The correlation of Miyara et al. [4], which was initially developed from R-22 and R-410A data inside a herringbone microfin tube, deviated from the measurements of this study on average by 7%, even though it was used to predict the pressure drops of not only R-22, but also R-407C and R-134a. This implied that this correlation could maybe be used for refrigerants other than R-22 and R-410A at higher mass fluxes.

An existing helical microfin tube correlation obtained from the literature was modified to predict the pressure drops inside the herringbone microfin tube. The results indicated that this modified correlation predicted the data within an average error of 1% and an average mean deviation of 6.8%.

Acknowledgments

Wolverine, Inc., Alabama, supplied the experimental helical microfin tubes, and Petur Thors is thanked for arranging the donation. Dr. Alex Kriegsmann of Wieland Werke also kindly donated several lengths of microfin tubing. The experimental herringbone microfin tube was donated by Professor Yasuyuki Takata of Ky-

ushu University, Japan, for which the authors are most grateful. The research work was performed with a South African National Research Foundation grant, under Grant No. 2053278.

Nomenclature

A = area
 D = diameter
 e = fin height
 Ft = Froude rate
 f = friction factor
 G = mass flux
 h = enthalpy
 L = length
 n = number of fins
 Δp = pressure drop
 PF = penalty factor
 Re = Reynolds number
 T = temperature
 t = thickness
 x = vapor quality
 X_{tt} = Lockhart-Martinelli parameter
 X, Y = constants, Eq. (16)

Greek Letters

β = helix angle
 ε = void fraction
 γ = apex angle
 ρ = density

Subscripts

b = base
 e = equivalent
 ex = experimental
 f = friction
 fa = actual flow
 g = gravitational
 h = herringbone
 he = helical
 i = inside, inlet
 L = liquid
 Lo = liquid only
 m = momentum
 n = nominal
 o = outside, outlet
 pd = predicted
 s = smooth
 V = vapor
 w = wall

References

- [1] Liebenberg, L., 2002, "A Unified Prediction Method for Condensation Performance in Smooth and Microfin Tubes," Ph.D. thesis, Rand Afrikaans University, Johannesburg.
- [2] Miyara, A., Otsubo, Y., Ohtsuka, S., and Mizuta, Y., 2003, "Effects of Fin Shape on Condensation in Herringbone Microfin Tubes," *Int. J. Refrig.*, **26**, pp. 417–424.
- [3] Ebisu, T., and Torikoshi, K., 1998, "Experimental Study on Evaporation and Condensation Heat Transfer Enhancement for R-407C Using Herringbone Heat Transfer Tube," *ASHRAE Trans.*, **104**(2), pp. 1044–1052.
- [4] Miyara, A., Nonaka, K., and Taniguchi, M., 2000, "Condensation Heat Transfer and Flow Pattern Inside a Herringbone-Type Microfin Tube," *Int. J. Refrig.*, **23**, pp. 141–152.
- [5] Goto, N., Inoue, N., and Ishiwatari, N., 2001, "Condensation and Evaporation Heat Transfer of R-410A inside Internally Grooved Horizontal Tubes," *Int. J. Refrig.*, **24**, pp. 628–638.
- [6] Kline, S. J., and McClintock, F. A., 1953, "Describing Uncertainties in Single-Sample Experiments," *Mech. Eng. (Am. Soc. Mech. Eng.)*, **75**, pp. 3–8.
- [7] REFPROP, 1999, "NIST Thermodynamic Properties of Refrigerants and Refrigerant Mixtures (REFPROP)," Version 6.0, *NIST Standard Reference Database 23*, National Institute of Standards and Technology, Gaithersburg, MD.
- [8] Rouhani, S. Z., and Axelsson, E., 1970, "Calculation of Volume Void Fraction in the Subcooled and Quality Region," *Int. J. Heat Mass Transfer*, **13**, pp. 383–393.

- [9] Thome, J. R., 2003, "On Recent Advances in Modeling of Two-Phase Flow and Heat Transfer," *Heat Transfer Engineering*, **24**(6), pp. 46–59.
- [10] Lockhart, R. W., and Martinelli, R. C., 1949, "Proposed Correlation of Data for Isothermal Two-Phase, Two-Component Flow in Pipe," *Chem. Eng. Prog.*, **45**, pp. 39–48.
- [11] Cavallini, A., Del Col, D., Doretti, L., Longo, G. A., and Rossetto, L., 2000, "Heat Transfer and Pressure Drop During Condensation of Refrigerants Inside Horizontal Enhanced Tubes," *Int. J. Refrig.*, **23**, pp. 4–25.
- [12] Owaga, D. C., 2003, "Flow Patterns during Refrigerant Condensation in Smooth and Enhanced Tubes," Master's dissertation, Rand Afrikaans University, Johannesburg.
- [13] Liebenberg, L., Thome, J. R., and Meyer, J. P., 2004, "Flow Pattern Identification With Power Spectral Density Distributions of Pressure Traces During Refrigerant Condensation in Smooth and Microfin Tubes," *ASME J. Heat Transfer*, submitted for review.
- [14] Wang, J., Lan, S., and Chen, G., 2000, "Experimental Study on the Turbulent Boundary Layer Flow Over Riblets Surface," *Fluid Dyn.*, **27**(4), pp. 217–229.
- [15] Carnavos, T. C., 1980, "Heat Transfer Performance of Internally Finned Tubes in Turbulent Flow," *Heat Transfer Eng.*, **4**(1), pp. 32–37.
- [16] Souza, A. L., and Pimenta, M. M., 1995, "Prediction of Pressure Drop During Horizontal Two-Phase Flow of Pure and Mixed Refrigerants," *ASME Conference on Cavitation and Multiphase Flow*, ASME, New York, Vol. 210, pp. 161–171.
- [17] Friedel, L., 1979, "Improved Friction Pressure Drop Correlation for Horizontal and Vertical Two-phase Two-component Flow in Pipes," E2, European Two-Phase Flow Group Meeting, Ispra.
- [18] Azer, N. Z., and Said, S. A., 1982, "Augmentation of Condensation Heat Transfer by Internally Finned Tubes and Twisted Tape Inserts," *Proc. of 7th Int. Heat Transfer Conference*, München, West-Germany, Hemisphere, **5**, pp. 33–38.
- [19] Haraguchi, H., Koyama, S., and Fujii, T., 1994, "Condensation of Refrigerants HCFC22, HFC134a and HCFC123 in a Horizontal Smooth Tube: 1st Report, Proposals of Empirical Expressions for the Local Frictional Pressure Drop," *Trans. JSME*, **60**, pp. 2111–2116.